PAPER • OPEN ACCESS

Open-source electronics ecosystem for optical atomic clocks

To cite this article: Piotr Morzyński *et al* 2023 *Meas. Sci. Technol.* **34** 075022

View the article online for updates and enhancements.

Open-source electronics ecosystem for optical atomic clocks

Piotr Morzyński*(ID)**, Sławomir Bilicki**(ID)**, Marcin Bober**(ID)**, Adam Ledziński,
Marcin Witkowski**(ID)**, Mehrdad Zarei**(ID) **and Michał Zawada**(ID)

Institute of Physics, Faculty of Physics, Astronomy and Informatics, Nicolaus Copernicus University,
Grudziądzka 5Grudzidzka 5, Toruń, PL-87-100, Poland

E-mail: pmorzynski@fizyka.umk.pl

CrossMark

Abstract
We present an open-source hardware and software ecosystem for optical atomic clocks. We provide PCB schematics and fabrication files for manufacturing the most important electronic systems together with the required software. The boards are designed for an active bad-cavity superradiant strontium clock and a passive optical lattice strontium clock, but they can be easily adapted to other atomic species' optical atomic clocks or ultra-cold atoms' systems like magneto-optical traps or Bose–Einstein condensate setups.

Keywords: active superradiant optical clock, electronic components, optical atomic clocks, rf electronics

(Some figures may appear in colour only in the online journal)

1. Introduction

Experimental systems in atomic, molecular and optical physics demand more and more complex and sophisticated requirements to see subtle effects like searching for dark matter [1, 2], Bose–Einstein condensates [3, 4], gravitational wave detection [5], spectroscopy of ultra-narrow transitions [6, 7] and other ultra-cold atom experiments [8, 9]. Among them, one of the most dominant examples is optical atomic clock experiments [6]. In realising such high-accuracy measurements, various non-standard solutions not available on the commercial market must be implemented. The most challenging is the design of electronic elements that can produce stable radio frequency or magnetic field pulses. Another common problem is adapting these devices to work with experiment control systems such as Sinara/ARTIQ [10]. Usually, a local electronic workshop is employed to prepare electronic devices

and systems that are unique to only one particular experiment within a group. With their unprecedented precision, optical atomic clocks need many custom-made components to drive experiments correctly. While most existing laboratories have developed their own solutions for operating complex optical clocks, there are few papers that report their electronic circuits in detail [11–14]. At the same time, autonomously operated optical atomic clocks are becoming more common and in demand for new technology applications [15–17] and the new definition of the SI second [18, 19].

In this paper, we present an electronic system aimed at supporting the operation of optical clocks. While the electronic components presented here are designed for optical atomic clocks, they are also suitable for many other types of ultra-cold atom experiments, such as Feshbach resonance spectroscopy [20], optically pumped magnetometers [21], cold atom gravimetry [22] and quantum computing [23]. The presented electronic devices are suitable for both present-generation passive optical lattice atomic clocks and future-generation continuous active optical clocks based on superradiance [24–27]. They are composed of high-current drivers for controlling the magnetic field coils, a relocking system for the lasers' frequency stabilisation, direct digital synthesizer controllers, a phase and frequency comparator for laser–laser

* Author to whom any correspondence should be addressed.

or laser–optical frequency comb (OFC) relative locks, and a cooling fluid flow-based interlock control circuit. Most of the presented devices can be configured using Ethernet and fast-switched using analog or transistor-transistor logic (TTL) signals. The designs are adapted to the electronic components currently available on the market.

All presented components are open-source hardware and software. In the open data repository we provide all PCB schematics and fabrication files required to manufacture the most important electronic systems together with the required software.

2. Components

2.1. Magneto-optical traps and offset field controller 15 A/100 A

Collecting atoms into optical lattices requires first laser cooling them down to several tens of μK temperatures. This is commonly performed in magneto-optical traps (MOTs) [28–30]. A quadrupole magnetic field, used in the MOT, is usually generated by a pair of anti-Helmholtz circular coils. Laser cooling and trapping of strontium are generally realised in two consecutive MOTs operating on two different atomic transitions [31, 32]. Therefore, two different values of current flowing through the coils need to be optimised in each of the MOTs, and ramping of the magnetic field gradients is required. This, together with fast turning on and off of the field, must be provided by the current controller.

Operating an optical lattice strontium clock after loading atoms into the lattice requires a static and homogeneous magnetic field either for defining a quantisation axis for the atoms and resolving clock transition hyperfine components needed for optical pumping and clock interrogation in fermionic ^{87}Sr isotope or for magnetic-induced spectroscopy [33] in the bosonic ^{88}Sr isotope [6].

The aforementioned conditions require the capability to switch the direction of the current in one of the coils to move from an anti-Helmholtz configuration to a Helmholtz configuration.

In the case of a passive optical lattice strontium clock, the presence of the magnetic field induces systematic shifts to the atomic clock line, such as first- and second-order Zeeman shifts. The achievable stability of the magnetic field determines the uncertainty of these systematic shifts and, thus, the clock's accuracy. Moreover, the fluctuations of the magnetic field will directly deteriorate the clock's stability.

In a first-order Zeeman shift, a magnetic field, B, gives a linear shift of the sub-levels, which for π-transitions ($\Delta m_F = 0$) shifts the transition frequency, f, by $\Delta f_{\text{lin}} = -m_F B (g_e - g_g) \mu_B / h$, where μ_B is the Bohr magneton and g_e and g_g are the g-factors of the excited and ground state, respectively. For ^{87}Sr, a linear Zeeman shift has been determined experimentally to be $\Delta f_{\text{lin}} = 1.084(4) m_F B$ Hz μT^{-1} [34].

A second-order Zeeman shift determination depends on the structure of the atomic levels, and in the case of strontium, the shift is dominated by the interaction of the excited triplet clock state with the other nearest triplet state, $\Delta f_{\text{quad}} \approx$

$-2B^2 \mu_B^2 / (3 \Delta \nu_t h^2)$, where $h \Delta \nu_t$ is the energy separation between the two triplet states.

For strontium, the quadratic Zeeman shift is $\Delta f_{\text{quad}} \approx -2.46 \times 10^{-5} B^2$ Hz μT^{-2} [35].

Assuming $B = 60$ μT in state-of-the-art ^{87}Sr clocks [35, 36] a fractional accuracy of 10^{-18} requires a stability of the B field better than $\Delta B < 0.000\,087$ μT, i.e. $\Delta B / B < 1.45 \times 10^{-6}$. For a bosonic ^{88}Sr clock, the bias field is usually higher, for instance $B = 210$ μT in one of the best transportable clocks [37]. There is, however, no linear Zeeman shift. The quadratic Zeeman shift sets the requirements $\Delta B < 0.04$ μT, i.e. $\Delta B / B < 1.9 \times 10^{-4}$.

In contrast to passive clocks, an active superradiant clock uses the radiation collected directly from the clock transition as a reference. The atoms are correlated in the superradiant emission, creating a collective atomic dipole. To a first approximation, superradiance may occur if the relative frequency shifts, δf, between atoms are below the atomic line width. The space and time inhomogeneity, δB, of the magnetic field applied to the ensemble of superradiating atoms leads to different frequency shifts of the upper lasing state. For the 1 mHz line of fermionic ^{87}Sr and a field of 60 μT the field's required space and time homogeneity due to the linear Zeeman shift is on the order of $\delta B / B \sim 3 \times 10^{-6}$. In the bosonic isotope ^{88}Sr the induced line width is extremely small and depends quadratically on the value of the offset field B [38]. For instance, $B = 200$ μT induces a line width of ∼1.2 nHz. Therefore, the quadratic Zeeman shift imposes extremely high space and time homogeneity requirements at the level of $\delta B / B \approx 10^{-9}$.

However, as was shown in [39], the superradiance of an atomic ensemble in a bad-cavity regime is allowed for less restrictive conditions, i.e. $\delta f < N g^2 / \kappa$, where N is the number of atoms, g is the coupling strength of the lasing transition with the cavity mode and κ is the decay rate of the cavity field. Based on this, one can estimate the required homogeneity of the magnetic field over the atomic ensemble. For instance, for 10^5 ^{88}Sr atoms collected in a cavity with a finesse of 10^5, the estimation yields $\delta B / B < 10^{-5}$.

A finite-element method simulation of the magnetic field homogeneity for a magnetic field generated from in-vacuum coils surrounded by Mu-metal shields is presented in figure 1. It shows that such homogeneity is possible even with the highly inhomogeneous field from MOT coils present just outside the shields. This particular setup is designed for an active continuous optical clock based on the idea of a moving magic-wavelength lattice scheme, as proposed in [26, 40].

The device presented schematically in figure 2 has two separate controllers, for currents up to 15 A and 100 A, respectively, to increase resolution in the low-current regime. The active controller is selected by a TTL signal. A block diagram of a controller is presented in figure 3 on the basis of the 100 A controller. An output current is set by analogue input. The analogue signal is converted to digital and digitally filtered to remove any input noise. A digital proportional-integral-derivative (PID) controller and a digital–analogue converter (DAC) stabilise the current output sensed by a LEM IT 200S Ultrastab current sensor. The digital–analogue converter is referenced to an external ultra-stable ADR4540BRZ voltage
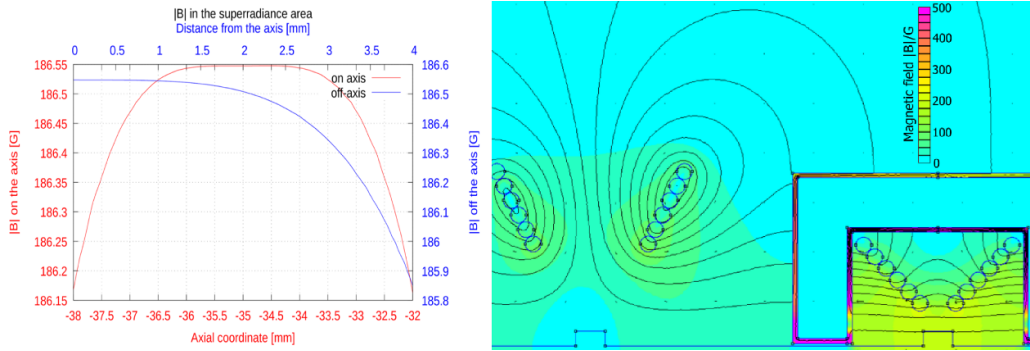
Figure 1. Magnetic field distribution simulations for the set of MOT field coils and bias field coils for the superradiance experiment. The superradiant area is surrounded by a magnetic shield. Left: Numerical simulations of the magnetic field in the area of superradiance performed for the following parameters: $I = 40$ A, six windings per coil, internal radius 8 mm, distance between coils 4 mm, copper wire thickness 3.175 mm, permeability of the shields 87 000, thickness of the shields 1 mm. The external magnetic field generated by the MOT coils has been taken into account. Right: Distribution of the magnetic field in the MOT and superradiance area (inside of a two-layer magnetic shield, shown in the bottom-right). Cross-sections of the Mu-metal shields and copper windings are visible.
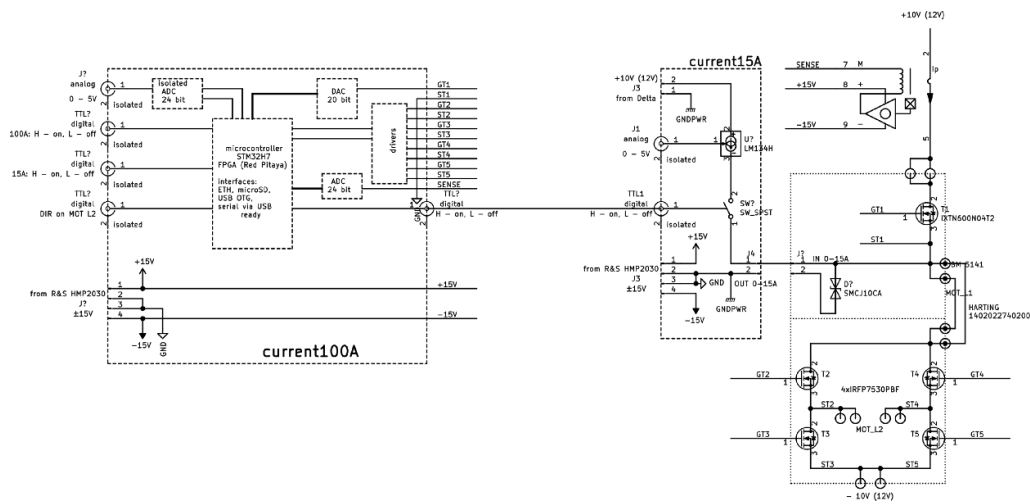

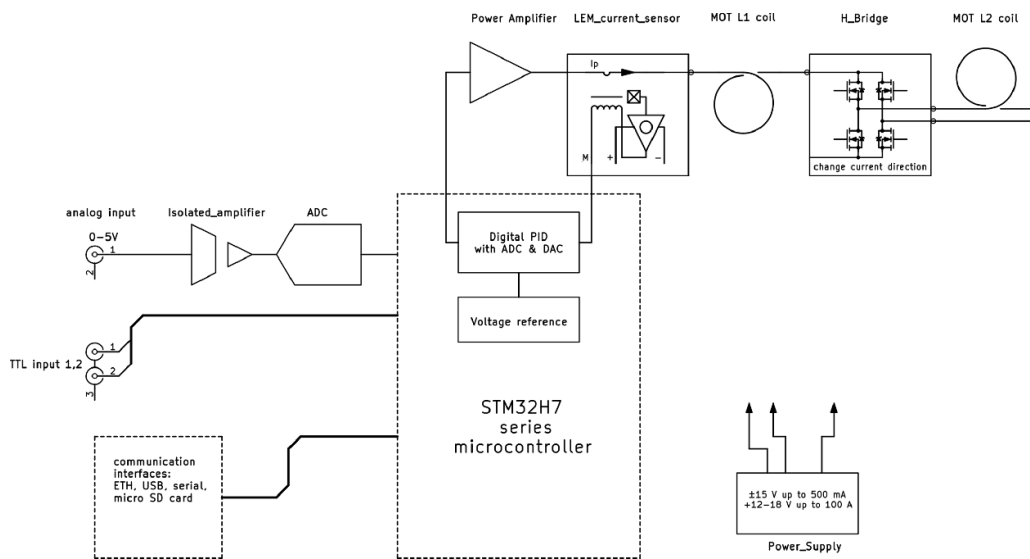**Figure 2.** Concept of 15 A/100 A current controller.
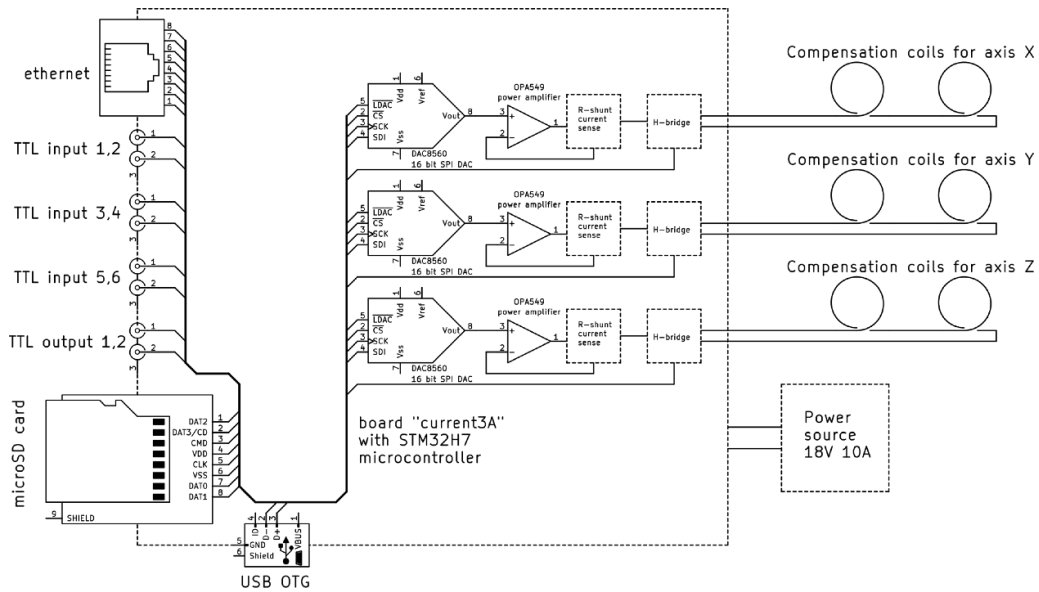

Figure 3. 100 A part of the current controller.

Figure 4. Compensation coils controller. © 2022 IEEE. Reprinted, with permission, from [44].

reference with the relative noise below 6.6×10^{-7} and relative temperature drift coefficient below $5 \times 10^{-7}\,^\circ\mathrm{C}^{-1}$. Both or only one of the coils can be connected by an H-bridge to allow changing of the current direction in both coils, or only in one of them, enabling switching between Helmholtz and anti-Helmhotz configurations. The full PCB schematics together with fabrication files for the PCB design and manufacturing are available at [41, 42].

2.2. Compensation coils controller (3×3A)

In any cold atom experiment, precise control over the magnetic field is necessary. It is especially important to have a 3D control to compensate for the Earth's magnetic field and any stray magnetic fields in the laboratory. On the other hand, transferring atoms between different traps, such as between a MOT and an optical lattice, is usually enhanced by adding static offset fields, for instance to compensate imbalances of laser light intensity in retro-reflected beams. Three pairs of different Helmholtz coils usually ensure all these conditions. Due to experimental space constraints, usually the pairs are not identical and require different currents.

The current controller for the compensation coils should be able to tune the currents' values and change their directions independently for each pair. Assuming that the Earth's and stray magnetic fields are below $100\,\mu\mathrm{T}$ in each direction, a fractional clock accuracy of 10^{-18} requires the same level of stability of the magnetic field as described in the previous section.

The presented device can be programmed by Ethernet connection over Telnet protocol. Programming allows presetting in memory 32 values of the current on each of the compensation coils. Fast addressing and setting the output values is performed by TTL signals (five addressing bits and one clock/set bit). An output in the range of -3 A to 3 A is

provided by a 16-bit digital–analogue converter stabilised to the ultra-stable ADR443BRZ voltage reference. Additionally, an arbitrary-length linear ramp can be programmed, triggered by a clock/set TTL.

A conceptual diagram is presented in figure 4. The full PCB schematics and fabrication files for the PCB design and manufacturing are available at [43]. For each channel, the current is stabilised to the digital–analogue converter output by sensing the current using high-quality shunt resistors. The coils are connected through a TTL-controlled H-bridge.

We also provide open-source software (see appendix A) that allows presetting up to eight values for the current, but it can be easily adapted to the full capabilities of the controller, including USB and microSD card inputs. The presented device is a continuation of our previous work reported in [44].

2.3. Autonomous relocking system

The operation of an optical clock depends on the simultaneous correct operation of many subsystems, including dozens of systems for precise stabilisation of the lasers' frequencies to external references such as spectrometers, optical cavities, OFCs and atomic lines. As a result of mechanical, thermal and electrical disturbances, laser controllers may lose their optimal working conditions and remain in a state that makes it impossible to maintain the lock, thus interrupting the clock's operation. The remedy for this type of issue is an electronic autonomous relocking system. Most of the time, their operation is based on continuous observation of selected signals, detecting an approaching unstable working condition and correcting the settings of the appropriate device, as necessary. However, if a loss of lock is detected, an attempt is made to restore the lock, and the event is added to a log.

In a real system, each laser has individual operating parameters, behaviours and relocking algorithms. Therefore, the
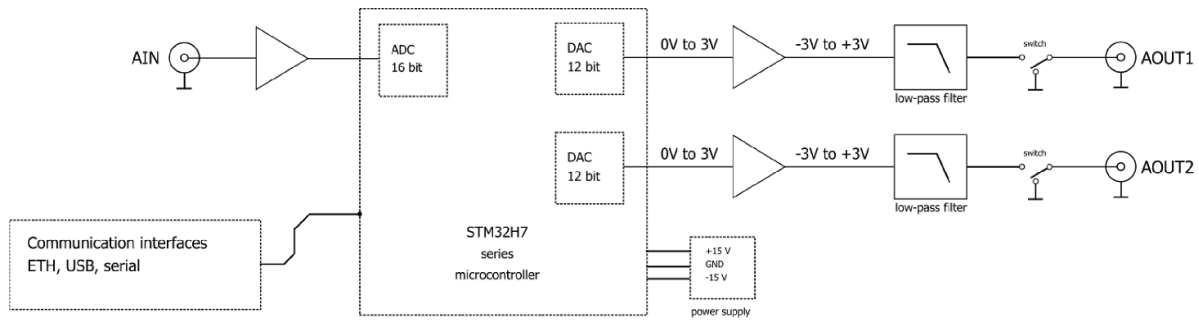
Figure 5. Relock board.

relocking device should be based on a programmable setup. Both the output and input signals could be analogue or digital (an example of digital input signals may be data from a wavelength meter or an OFC); therefore, analog to digital converters (ADC) and digital to analog converters (DAC) are required as well as digital communication ports.

We have developed a compact ADC/DAC card compatible with a Nucleo-H743ZI2 board (figure 5). By default the card is adapted to work with Toptica external cavity diode laser (ECDL) drivers, but it may also be used with other devices. The card requires a $+/-15$ V power supply delivered from the controlled device to avoid electrical disturbances. The signal from the analogue input port is amplified and directly connected to the built-in microcontroller 16-bit ADC converter. The input signal is used to observe transmission through the optical cavity and detect the loss of a lock by the signal falling to zero. When used with an injection-locking system [45], the transmission signal can be observed through an optical filter. It can also be used to monitor for single/multi-mode laser operation when used with a Fabry–Pérot interferometer. The analogue output signal is generated by the built-in microcontroller DAC converter, and then, with the use of operation amplifiers, the range of generated voltages is extended to -3 V to 3 V instead of the 0 V to 3 V range produced by the microcontroller. Operating around zero voltage is of great practical importance and allows the device to be easily switched from automatic to manual operation. The board is equipped with manual switches allowing for smooth connection and disconnection to an already working laser driver. Output analogue signals are usually used for slow compensation of laser diode current or external cavity piezo voltages with modulation ports on the laser drivers, which are very sensitive to any electrical noise. For this reason, a low-pass filter is used to cut potential high-frequency noise derived from the DAC.

The Nucleo-H743ZI2 board is equipped with an Ethernet communication port, which extends the functionality of the relock board. The board can act as a remote DAC and ADC controlled via a local network if the relocking algorithm is run on a computer in the lab. On the other hand, the relocking program (written in the C language) can be run on the microcontroller, making the system autonomous. In this case, Ethernet connectivity is very useful, for example if data from a wavelength meter is required.

The complete PCB schematics and fabrication files for the PCB design and manufacturing are available at [46].

2.4. Direct digital synthesizer controller

Many parts of optical clocks require precise control of the laser frequency. This is especially important in clock transition spectroscopy, for capturing cold atoms in optical traps, when operating on the magic wavelength, for frequency transfer and for conversion from the optical to the RF domain. For all of these tasks, acousto-optical modulators or electro-optical modulators driven by RF generators are used. Therefore, precise frequency generators are essential. For the best performance, the resolution of the frequency control should be on the order of the µHz level, with the possibility to use an external precise clock, such as a H-maser, as a reference. It is often required to switch between different frequencies in a short time (i.e. less than 1 µs) and to have the ability to change parameters by other programs via a LAN network. Most of the frequency generators available on the market do not meet all these requirements, and custom solutions are needed. Commercial direct digital synthesizer evaluation boards from Analog Devices (such as the AD9912 or AD9959) have proven to be a good choice. However, they need to be controlled via fast serial peripheral interface (SPI) interfaces.

We have developed a compact module compatible with the AD9959 and AD9912 evaluation boards based on a microcontroller, which significantly extends the capabilities of these boards, makes them easier to use and has the vast majority of the functionality needed in an optical atomic clock laboratory. A schematic of the device is presented in figure 6. The module communicates with the direct digital synthesizer (DDS) board via the fast SPI. It is equipped with an Ethernet port, allowing easy control of the device from anywhere in the laboratory (see appendix B). Analogue and digital ports can be used, among others, for reading the voltage from a photodetector, fast switching of RF signal parameters using TTL signals, quick switching of other clock modules and for synchronisation. Different algorithms useful in optical clocks have been implemented in the microcontroller, such as a digital lock to the spectral profile, scanning a spectral profile, optical cavity linear drift cancellation and fast switching between different RF frequencies triggered by a TTL signal, with the option
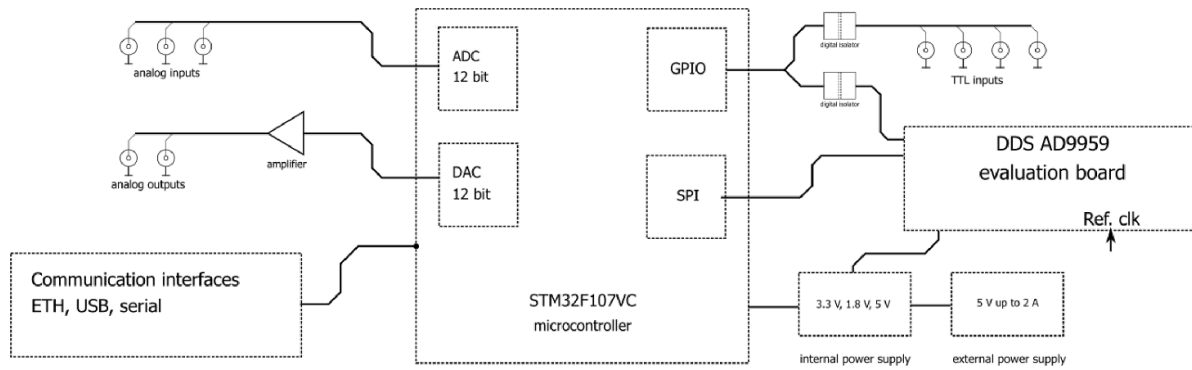
Figure 6. Block diagram of the direct digital synthesizer controller.

of soft switching using a ramp. The module requires a 5 V power supply and provides all the necessary power for the DDS board. If a homemade 1 GHz voltage-controlled crystal oscillator (VCXO) is used as the external reference clock signal, the device may be used as a voltage-controlled generator with digitally tunable centre frequency. Such functionality is often used for fibre noise cancellation [47, 48].

The full PCB schematic of the comparator, together with the required fabrication files for manufacturing and software for the microcontroller, are available at [49, 50].

2.5. Phase and frequency comparator with frequency divider

A phase and frequency comparator is an indispensable component whenever the laser beam frequency stabilisation step employs beat-note detection and a phase-locking setup. In passive optical atomic clocks this includes stabilisation of lasers to an OFC [51, 52], phase stabilisation between two lasers by optical offset phase locking [53, 54] and active Doppler shift cancellation in optical fibres [47, 48].

In an active optical clock based on superradiance, a phase and frequency comparator is necessary to provide the length stabilisation of the superradiant cavity. To achieve superradiance conditions in a bad-cavity regime, one of the optical cavity modes has to be tuned to the atomic transition frequency. A superradiant cavity that can sustain superradiance in both fermionic ^{87}Sr and bosonic ^{88}Sr isotopes of strontium requires a finesse on the order of 100 000. Assuming a length of 15 cm, the full width at half maximum of the cavity mode is 5 kHz. This implies that the frequency of the chosen mode of the cavity has to be tuned and stabilised with a precision of 1 kHz or better. The cavity mode frequency is determined by the cavity length, and the length, in turn, can be locked to some external laser [55] with absolute frequency stability. Tuning can then be achieved with an acousto-optic modulator (AOM) and stabilisation to an external reference, such as the OFC.

A simple offset lock for the laser frequency to an OFC is depicted in figure 7. An error signal for laser stabilisation is generated by comparing the phase difference between a stable RF generator and an optical beat note between the OFC tooth and the laser. A phase difference detection is made by a phase and frequency comparator with a variable dividing the ratio of the input frequency signal. This frequency divider allows adjustment of the sensitivity of the system. The generated error signal is applied through a PID controller to the laser.

A schematic diagram of a comparator is presented in figure 8. A digital phase frequency detector (HMC439QS16G), used in our comparator, provides an output voltage proportional to the phase difference between the inputs when this difference is smaller than $\pm\pi$. For higher phase differences, the output voltage saturates at the positive or negative value, depending on which input frequency is higher. This particular property provides a high capture range for the lock system. The values of the frequency dividers are set over a SPI from a simple microcontroller. The microcontroller itself is programmed manually by two arrays of jumpers. The full PCB schematic of the comparator together with the required fabrication files for manufacturing and software for the microcontroller are available at [56].

2.6. Water flow sensor interlock

In both active and passive optical atomic clocks, the high-current coils require water cooling. This includes MOTs and offset coils, and the Zeeman slower coils if not based on permanent magnets. Overheating of these coils can be catastrophic to the experiment. An interlock control circuit verifying the returning water flow provides an instantaneous fail-safe protection by turning off the power supply.

Figure 9 presents a diagram of the device. The interlock control's design is kept simple on purpose, and any faults in its operation should switch off the power supply to prevent overheating of the coils. Flow sensor impulses are converted to voltage, and this voltage is compared by a differential amplifier with a pre-adjusted discriminating level. The output of the differential amplifier is sent through a flip-flop latch to a relay that changes the interlock state in a power supply. If the flow drops below the discriminated level, the latch will cut the power to the relay, and will not bring it back online before a human operator checks the system and resets the flip-flop latch. The complete PCB schematic of the interlock sensor together with the required fabrication files for manufacturing are available at [57].
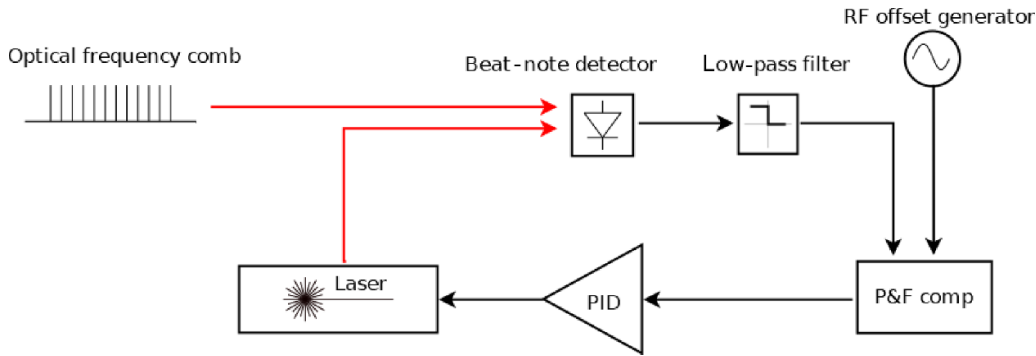
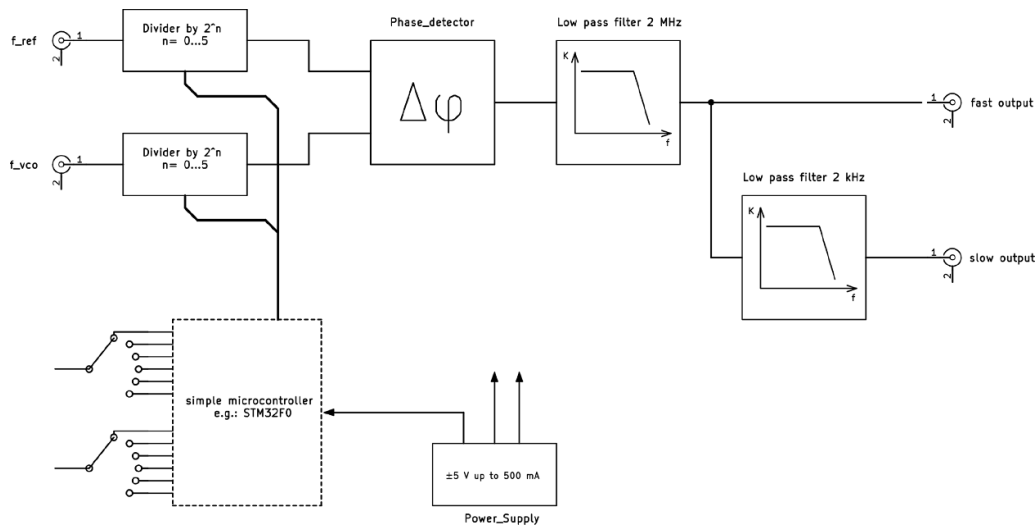**Figure 7.** A simple offset lock to an optical frequency comb with a phase and frequency comparator.

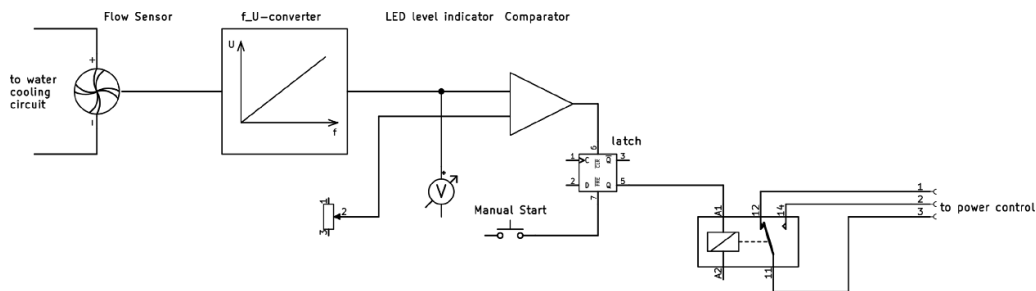**Figure 8.** Phase and frequency comparator.

Figure 9. Diagram of a flow sensor interlock.

3. Conclusions

In this paper, we detail an open-source hardware and software ecosystem designed for optical atomic clocks. These designs include a wide range of electronic circuits optimised for precision control of magnetic fields (controllers up to 100 A and compensation coils), maintaining and distribution of frequencies (relocking system for lasers, DDS controller, phase and frequency comparator), and for water cooling (water flow sensor interlock). The presented systems allow us to meet the challenging conditions required in passive and superradiant active optical atomic clocks. They are also suitable for many other ultra-cold atom experiments.

Data availability statement

The data that support the findings of this study are openly available from the following sources: [41–43, 46, 49, 50, 56, 57].

Acknowledgment

Appendix A. Software for the compensation coils driver

The compensation coils driver is programmed by presetting into its memory the values of the output currents over the Telnet protocol. During operation, the output currents can be changed between preset values by input TTL signals. This method is compatible with DIO cards and RT computers used in the laboratory environment to control experiments. Additional parameters stored in the memory together with current values allow either fast switching between desired levels or a linear ramp of arbitrary time.

A.1. Pre-programming memory

The format of commands used in Telnet programming is

$< parameter\ address >: \quad < value1 >; \quad < value2 >;$
$< value3 >; \quad < time >$

where *'parameter address'* sets the logical address in the memory , *'valueX'* are the preset current values for the respective coils, and *'time'* is the length of a linear ramp in milliseconds; a value of 1 means the fastest possible switching.

Multiple parameters may be set with a single command by separating them with an '&' sign:

$< parameter\ address >: \quad < value1 >; \quad < value2 >;$
$< value3 >; \quad < time >; \quad \& < address >: \quad < value1 >;$
$< value2 >; \quad < value3 >; \quad < time >; \quad \& \quad \dots$

Two additional commands may used to get help and to close the connection:

```
help
exit
```

The most common parameters and addresses are presented below:

DAC: 000	set values for memory 1
DAC: 001	set values for memory 2
DAC: 010	set values for memory 3
000	address of memory 1
001	address of memory 2
010	address of memory 3

After making a connection, if the connection is successful a help message will be sent by the driver. This message guides the operator how to communicate with the driver. For example, the command to pre-program the first two memory values is

```
DAC: 000: −1.25 684; 0.5; 0.0; 1; & 001:
0.52; −2.1; −1.0; 50;
```

Switching to the first memory (000) levels takes 1 ms, while switching to the second memory levels (001) is made using a 50 ms long linear ramp.

A.2. Switching between pre-programmed levels

In the current version of the software, switching between pre-programmed values is made by four TTL signals, but it can be easily expanded to use all six available TTL inputs. Three TTL signals address the required memory, and one TTL is a set/clock signal that triggers switching outputs to the new memory levels. TTL 1 is the least significant bit, and TTL 3 is the most significant bit [44].

For instance, the following pattern switches the controller output to the pre-programmed value stored in memory location 2 (001).

TTL 1	TTL 2	TTL 3	TTL 4
1	0	0	⊓

Appendix B. Software for dds

The device is controlled by setting the appropriate parameters using the Telnet protocol. The format for writing the parameters is

$< parameter\ name > \quad < value >.$

Multiple parameters may be set in one command by separating them with a ';' sign:

$< parameter\ name > \quad < value >; < parameter\ name >$
$< value >; \dots.$

The command bellow is used to read the value of a parameter:

$< parameter\ name >?$

The most common commands are presented below:

DDS:CH0:FREQ	set frequency of the ch0 dds output (value in MHz)
DDS:CH0:AMP	set amplitude of the ch0 dds output (value from 0 to 1)
DDS:CH0:PH	set phase of the ch0 dds output (value in deg)
SCAN:ON	turn on/off (value 1/0) the frequency scan
SCAN:RANGE	scan range in MHz
SCAN:STEP	scan step in MHz
SCAN:CH	the number of the dds output channel on which the scan is performed
SCAN:GNDCMP	turn on/off (value 1/0) removing background form spectroscopy (additional setup driven by TTL for turnning on and off the signal required)
SCAN:VOLT	the value of the measured signal (value in bits of ADC)
SCAN:DT	dead time between setting the frequency and measurement
DLOCK:ON	turn on/off (value 1/0) digital lock
DLOCK:JUMP	amplitude of frequency detuning for digital lock
ADC:CH0:AVR	number of ADC measurements executed for voltage measurement (the value is an average of ADC measurements)

For each of the parameters, apart from the value, one can set the maximum and minimum value and enable saving of the parameter values to the microcontroller memory with the following commands:

< `parameter name` > :MAX: maximum allowable value of the parameter.

< `parameter name` > :MIN: minimum allowable value of the parameter.

< `parameter name` > :TABON: turn on/off (value 1/0) saving data to memory.

< `parameter name` > :MES:SIZE: size of the table in memory.

ORCID iDs

Piotr Morzyński ⓘ https://orcid.org/0000-0001-6178-0934
Sławomir Bilicki ⓘ https://orcid.org/0000-0002-3914-4680
Marcin Bober ⓘ https://orcid.org/0000-0002-4773-6870
Marcin Witkowski ⓘ https://orcid.org/0000-0002-6875-308X
Mehrdad Zarei ⓘ https://orcid.org/0000-0002-9541-9829
Michał Zawada ⓘ https://orcid.org/0000-0002-2826-5129

References

[1] Wcisło P *et al* 2018 New bounds on dark matter coupling from a global network of optical atomic clocks *Sci. Adv.* **4** eaau4869

[2] Roberts B M *et al* 2020 Search for transient variations of the fine structure constant and dark matter using fiber-linked optical atomic clocks *New J. Phys.* **22** 093010

[3] Cornell E A and Wieman C E 2002 Nobel lecture: bose-einstein condensation in a dilute gas, the first 70 years and some recent experiments *Rev. Mod. Phys.* **74** 875

[4] Ketterle W 2002 Nobel lecture: When atoms behave as waves: bose-einstein condensation and the atom laser *Rev. Mod. Phys.* **74** 1131

[5] Abbott B P *et al* (LIGO Scientific Collaboration and Virgo Collaboration) 2016 Observation of gravitational waves from a binary black hole merger *Phys. Rev. Lett.* **116** 061102

[6] Ludlow A D, Boyd M M, Ye J, Peik E and Schmidt P O 2015 Optical atomic clocks *Rev. Mod. Phys.* **87** 637

[7] Derevianko A and Katori H 2011 Colloquium: physics of optical lattice clocks *Rev. Mod. Phys.* **83** 331

[8] Escudero R G, Chen C-C, Bennetts S, Pasquiou B and Schreck F 2021 Steady-state magneto-optical trap of fermionic strontium on a narrow-line transition *Phys. Rev. Res.* **3** 033159

[9] Ciamei A, Bayerle A, Chen C-C, Pasquiou B and Schreck F 2017 Efficient production of long-lived ultracold sr$_2$ molecules *Phys. Rev.* A **96** 013406

[10] Sinara 2023 Sinara Open Hardware Project (available at: https://sinara-hw.github.io/)

[11] Dobosz J, Bocheński M and Semczuk M 2021 Bidirectional, analog current source benchmarked with gray molasses-assisted stray magnetic field compensation *Appl. Sci.* **11** 10474

[12] Kobayashi T, Akamatsu D, Hosaka K and Yasuda M 2019 A relocking scheme for optical phase locking using a digital circuit with an electrical delay line *Rev. Sci. Instrum.* **90** 103002

[13] Subhankar S, Restelli A, Wang Y, Rolston S L and Porto J V 2019 Microcontroller based scanning transfer cavity lock for long-term laser frequency stabilization *Rev. Sci. Instrum.* **90** 043115

[14] Barker D S, Pisenti N C, Restelli A, Scherschligt J, Fedchak J A, Campbell G K and Eckel S 2019 A flexible, open-source radio-frequency driver for acousto-optic and electro-optic devices (arXiv:1908.02156)

[15] Stuhler J *et al* 2021 Opticlock: transportable and easy-to-operate optical single-ion clock *Meas. Sensors* **18** 100264

[16] Schuldt T *et al* 2021 Optical clock technologies for global navigation satellite systems *GPS Solut.* **25** 83

[17] Grotti J *et al* 2018 Geodesy and metrology with a transportable optical clock *Nat. Phys.* **14** 437

[18] Riehle F, Gill P, Arias F and Robertsson L 2018 The CIPM list of recommended frequency standard values: guidelines and procedures *Metrologia* **55** 188

[19] BIPM 2021 Recommended values of standard frequencies (available at: www.bipm.org/en/publications/mises-en-pratique/standard-frequencies)

[20] Thomas R and Kjærgaard N 2020 A digital feedback controller for stabilizing large electric currents to the ppm level for feshbach resonance studies *Rev. Sci. Instrum.* **91** 034705

[21] Jaufenthaler A, Kornack T, Lebedev V, Limes M E, Körber R, Liebl M and Baumgarten D 2021 Pulsed optically pumped magnetometers: addressing dead time and bandwidth for the unshielded magnetorelaxometry of magnetic nanoparticles *Sensors* **21** 1212

[22] Wang H *et al* 2022 A truck-borne system based on cold atom gravimeter for measuring the absolute gravity in the field *Sensors* **22** 6172

[23] Young A W, Eckner W J, Milner W R, Kedar D, Norcia M A, Oelker E, Schine N, Ye J and Kaufman A M 2020

Half-minute-scale atomic coherence and high relative stability in a tweezer clock *Nature* **588** 408

[24] Meiser D, Ye J, Carlson D R and Holland M J 2009 Prospects for a millihertz-linewidth laser *Phys. Rev. Lett.* **102** 163601

[25] Chen C-C, Bennetts S, Escudero R G, Pasquiou B and Schreck F 2019 Continuous guided strontium beam with high phase-space density *Phys. Rev. Appl.* **12** 044014

[26] Kazakov G A and Schumm T 2013 Active optical frequency standard using sequential coupling of atomic ensembles *Phys. Rev.* A **87** 013821

[27] Norcia M A, Winchester M N, Cline J R K and Thompson J K 2016 Superradiance on the millihertz linewidth strontium clock transition *Sci. Adv.* **2** e1601231

[28] Phillips W D 1998 Nobel lecture: laser cooling and trapping of neutral atoms *Rev. Mod. Phys.* **70** 721

[29] Cohen-Tannoudji C N 1998 Nobel lecture: manipulating atoms with photons *Rev. Mod. Phys.* **70** 707

[30] Chu S 1998 Nobel lecture: the manipulation of neutral particles *Rev. Mod. Phys.* **70** 685

[31] Katori H, Ido T, Isoya Y and Kuwata-Gonokami M 1999 Magneto-optical trapping and cooling of strontium atoms down to the photon recoil temperature *Phys. Rev. Lett.* **82** 1116

[32] Loftus T H, Ido T, Ludlow A D, Boyd M M and Ye J 2004 Narrow line cooling: finite photon recoil dynamics *Phys. Rev. Lett.* **93** 073003

[33] Taichenachev A V, Yudin V I, Ovsiannikov V D, Pal'chikov V G and Oates C W 2008 Frequency shifts in an optical lattice clock due to magnetic-dipole and electric-quadrupole transitions *Phys. Rev. Lett.* **101** 193601

[34] Boyd M M, Zelevinsky T, Ludlow A D, Blatt S, Zanon-Willette T, Foreman S M and Ye J 2007 Nuclear spin effects in optical lattice clocks *Phys. Rev.* A **76** 022510

[35] Bothwell T, Kedar D, Oelker E, Robinson J M, Bromley S L, Tew W L, Ye J and Kennedy C J 2019 JILA SrI optical lattice clock with uncertainty of 2.0×10^{-18} *Metrologia* **56** 065004

[36] Takamoto M, Ushijima I, Ohmae N, Yahagi T, Kokado K, Shinkai H and Katori H 2020 Test of general relativity by a pair of transportable optical lattice clocks *Nat. Photon.* **14** 411

[37] Origlia S *et al* 2018 Towards an optical clock for space: Compact, high-performance optical lattice clock based on bosonic atoms *Phys. Rev.* A **98** 053443

[38] Taichenachev A V, Yudin V I, Ovsiannikov V D, Pal'chikov V G and Oates C W 2008b Frequency shifts in an optical lattice clock due to magnetic-dipole and electric-quadrupole transitions *Phys. Rev. Lett.* **101** 193601

[39] Kazakov G A and Schumm T 2017 Stability analysis for bad cavity lasers using inhomogeneously broadened spin-1/2 atoms as a gain medium *Phys. Rev.* A **95** 023839

[40] Kazakov G A and Schumm T 2014 Active optical frequency standards using cold atoms: perspectives and challenges

2014 European Frequency and Time Forum (EFTF) pp 411–4

[41] Ledziński A 2022 MOT and offset magnetic fields coils 100 A current controller RepOD (https://doi.org/10.18150/CAEGTJ)

[42] Ledziński A 2022 MOT and offset magnetic fields coils 15 A current controller RepOD (https://doi.org/10.18150/0MJ6GO)

[43] Ledziński A and Zarei M 2022 Compensation coils current controller (3x03A) RepOD (https://doi.org/10.18150/YHSPTP)

[44] Zarei M, Ledzinski A, Bober M, Zawada M and Morzynski P 2022 Automatic real-time control of magnetic field in an optical atomic clock *2022 Joint Conf. European Frequency and Time Forum AndIEEE Int. Frequency Control Symp. (EFTF/IFCS)* (IEEE)

[45] Stover H L and Steier W H 1966 Locking of laser oscillators by light injection *Appl. Phys. Lett.* **8** 91

[46] Ledziński A and Morzyński P 2022 Laser frequency stabilisation re-lock board RepOD (https://doi.org/10.18150/G2FT3P)

[47] Bergquist J, Itano W and Wineland D 1994 Laser stabilization to a single ion

[48] Ma L-S, Jungner P, Ye J and Hall J L 1994 Delivering the same optical frequency at two places: accurate cancellation of phase noise introduced by an optical fiber or other time-varying path *Opt. Lett.* **19** 1777

[49] Ledziński A 2022 DDS AD9912 single channel controller RepOD (https://doi.org/10.18150/YCLR91)

[50] Morzyński P 2022 DDS AD9959 four channel controller RepOD (https://doi.org/10.18150/GCW9EQ)

[51] Jost J D, Hall J L and Ye J 2002 Continuously tunable, precise, single frequency optical signal generator *Opt. Express* **10** 515

[52] Schibli T R, Hartl I, Yost D C, Martin M J, Marcinkevičius A, Fermann M E and Ye J 2008 Optical frequency comb with submillihertz linewidth and more than 10 w average power *Nat. Photon.* **2** 355

[53] Kumagai M, Kanamori H, Matsushita M and Kato T 1999 Development of phase-lock system between two single-mode lasers for optical-optical double resonance spectroscopy *Jpn. J. Appl. Phys.* **38** 6102

[54] Cygan A, Lisak D, Morzyński P, Bober M, Zawada M, Pazderski E and Ciuryło R 2013 Cavity mode-width spectroscopy with widely tunable ultra narrow laser *Opt. Express* **21** 29744

[55] Drever R W P, Hall J L, Kowalski F V, Hough J, Ford G M, Munley A J and Ward H 1983 Laser phase and frequency stabilization using an optical resonator *Appl. Phys.* B **31** 97

[56] Ledziński A and Morzyński P 2022 Phase and frequency comparator RepOD (https://doi.org/10.18150/SZEQYO)

[57] Ledziński A 2022 Water flow interlock RepOD (https://doi.org/10.18150/ZDZQD3)